

Original Article

Insulin resistance is associated with specific gut microbiota in appendix samples from morbidly obese patients

Isabel Moreno-Indias^{1,2*}, Lidia Sánchez-Alcoholado^{1*}, Eduardo García-Fuentes^{2,3}, Fernando Cardona^{1,2}, Maria Isabel Queipo-Ortuño^{1,2*}, Francisco J Tinahones^{1,2}

¹Clinical Management Unit of Endocrinology and Nutrition, Laboratory of The Biomedical Research Institute of Malaga (IBIMA), Virgen de la Victoria University Hospital, Malaga University, Malaga, Spain; ²Biomedical Research Networking Center for Pathophysiology of Obesity and Nutrition, Madrid, Spain; ³Clinical Management Unit of Endocrinology and Nutrition, Biomedical Research Institute of Malaga (IBIMA), Regional University Hospital, Malaga, Spain. *Equal contributors.

Received June 14, 2016; Accepted November 6, 2016; Epub December 15, 2016; Published December 30, 2016

Abstract: Alterations in intestinal microbiota composition could promote a proinflammatory state in adipose tissue that is associated with obesity and insulin resistance. Our aim was to identify the gut microbiota associated with insulin resistance in appendix samples from morbidly obese patients classified in 2 groups, high (IR-MO) and low insulin-resistant (NIR-MO), and to determine the possible association between these gut microbiota and variables associated with insulin resistance and the expression of genes related to inflammation and macrophage infiltration in adipose tissue. Appendix samples were obtained during gastric bypass surgery and the microbiome composition was determined by 16S rRNA pyrosequencing and bioinformatics analysis by QIIME. The Chao and Shannon indices for each study group suggested similar bacterial richness and diversity in the appendix samples between both study groups. 16S rRNA pyrosequencing showed that the IR-MO group had a significant increase in the abundance of *Firmicutes*, *Fusobacteria*, *Pseudomonaceae*, *Prevotellaceae*, *Fusobacteriaceae*, *Pseudomonas*, *Catenibacterium*, *Prevotella*, *Veillonella* and *Fusobacterium* compared to the NIR-MO group. Moreover, in the IR-MO group we found a significant positive correlation between the abundance of *Prevotella*, *Succinivibrio*, *Firmicutes* and *Veillonella* and the visceral adipose tissue expression level of IL6, TNF alpha, ILB1 and CD11b respectively, and significant negative correlations between the abundance of *Butyrivibrio* and *Bifidobacterium*, and plasma glucose and insulin levels, respectively. In conclusion, an appendix dysbiosis occurs in IR-MO patients, with a loss of butyrate-producing bacteria, essential to maintenance of gut integrity, together with an increase in mucin-degrading bacteria and opportunistic pathogens. The microbiota present in the IR-MO group were related to low grade inflammation in adipose tissue and could be useful for developing strategies to control the development of insulin resistance.

Keywords: Microbiota, appendix, insulin resistance, gut integrity, inflammation, adipose tissue

Introduction

Obesity is characterized by chronic subclinical inflammation that affects insulin activity in metabolically sensitive tissues (liver, muscle and adipose tissues) [1]. Recent studies in the past ten years have shown that this metabolic inflammation is characterized by a moderate excess in cytokine production, including interleukin (IL) IL-6, IL-1 or tumor necrosis factor alpha (TNF alpha), that injures cellular insulin signals and contributes to insulin resistance and diabetes [2, 3]. Recent research has high-

lighted links between the gut microbiota, obesity and insulin resistance [1, 4-7]. Growing evidence suggests that the gut microbiota contribute to host metabolism through communication with adipose tissue, which influences the development of metabolic alterations associated with obesity [8].

The intestinal microbiota have been shown to influence intestinal permeability in obese mice, thereby promoting translocation of bacterial products and stimulating the low-grade inflammation characteristic of obesity and insulin

resistance [9, 10]. Verdam et al. showed that the human obesity-associated microbiota profile is associated with local and systemic inflammation, although they did not find an association between the obesity-related microbiota composition and intestinal permeability, suggesting that the obesity-related microbiota composition has a proinflammatory effect [11].

The physiologic function of the human appendix is largely unknown but several hypotheses involve interactions between the abundant lymphoid tissue in the appendix and the microbiota contained within the appendix [12, 13]. In a recent study Guinane et al. concluded that the human appendix, although sharing a substantial amount of microbes with the intestinal tract, has its own defined microbiome. This microbial composition of the human appendix is subject to extreme variability and comprises a diversity of microbiota that may play an important role in human health [14]. The microbiota in appendix samples are a reflection of the microbiota present in the small intestine, which play an important role in host immunity and metabolism. In a preliminary study using polymerase chain reaction denaturing gradient gel electrophoresis (PCR-DGGE) we reported that intestinal bacterial DNA is a signature of insulin action in humans, but we did not identify the gut microbes associated with the insulin resistance phenotype [15].

The aim of the present study was to identify, using next-generation sequencing technologies, the precise gut microbiota associated with insulin resistance in appendix samples from morbidly obese patients, to provide a gut microbial signature for this phenotype, and also to determine the possible relationship between these gut microbiota and variables associated with insulin resistance and the expression of genes related to inflammation and macrophage infiltration in adipose tissue.

Material and methods

The homeostasis model assessment of insulin resistance (HOMA-IR) was used to classify the morbidly obese female patients. Specifically, patients with a HOMA-IR score of <3 were considered to comprise the low-insulin-resistant (NIR-MO) group, according to the mean \pm 2SD of a healthy control population. The morbidly obese patients with a HOMA-IR score of >7 were considered to be from the high insulin-resistant (IR-MO) group. Appendix samples

from 5 IR-MO and 5 NIR-MO patients matched for body mass index (BMI), age, gender, race and dietary intake were obtained during bariatric surgery. The samples were washed, fragmented, and frozen in liquid nitrogen before being stored at -80°C . All subjects were of Caucasian origin with no systemic disease or infection during the month before the study. Liver disease and thyroid dysfunction were specifically excluded by biochemical work-up. Other patient exclusion criteria included type 2 diabetes mellitus treated with insulin or oral antidiabetics, cardiovascular disease in the 6 months prior to study inclusion, arthritis, evidence of acute or chronic inflammatory disease, infectious diseases, or receiving drugs that could alter the lipid profile or the metabolic parameters at the time of inclusion in the study, renal involvement, history of drug or alcohol abuse (defined as 80 g/day), or serum transaminase activity more than twice the upper limit of normal, and the patient's decision not to participate in the study. The patients had not received any antibiotic, probiotic, or prebiotic agents in the 3-month period before the collection of appendix samples. The subjects were invited to participate by the Endocrinology Service of the Virgen de la Victoria Hospital (Malaga, Spain). Written informed consent was obtained in all cases and the protocol was approved by the Ethics Committee of Virgen de la Victoria Hospital.

Dietary assessment

A very-low-energy diet (Optifast® VLCD, Nestlé Health Science, Spain) was consumed by all the patients for a period of 8 weeks before gastric bypass surgery. Subjects ingested 3 shakes/day of Optifast®, which provided 456 kcal, 52 g protein, 7 g fat, and 45 g carbohydrates plus the recommended daily intake of vitamins, minerals, and trace elements. The patients were also permitted to eat other low-calorie foodstuffs (such as low-starch vegetables) to provide a total energy intake of 800 kcal/day. The dietary requirements were outlined by a dietitian before commencement of the diet, and all subjects attended for dietary counseling fortnightly thereafter. Any adverse effects of the diet were noted.

Analysis of biochemical variables

Blood samples were collected after an overnight fast. The serum was separated in aliquots

and immediately frozen at -80°C . Serum levels of glucose, cholesterol, triglycerides and HDL cholesterol were analyzed using a Dimension autoanalyzer (Dade Behring Inc., Deerfield, IL) by enzymatic methods (Randox Laboratories Ltd., UK). LDL cholesterol was calculated from the Friedewald equation. Gamma-glutamyl transpeptidase (GGT), glutamate-oxaloacetate transaminase (GOT), and glutamic pyruvic transaminase (GPT) (Wako Bioproducts, Richmond, VA, USA) were all measured by standard enzymatic methods. Additionally, insulin was quantified by RIA provided by BioSource S.A. (Nivelles, Belgium). High-sensitivity C-reactive protein (CRP) levels were measured by ELISA kit from BLK Diagnostics (Badalona, Spain). Leptin and adiponectin were analyzed by enzyme immunoassay (ELISA) kits (DSL, Webster, TX, and DRG Diagnostics GmbH, Germany, respectively). Glucagon-like peptide-1 (GLP-1) was measured by a human GLP-1 enzyme immunoassay (EIA) kit from Phoenix Pharmaceuticals (Karlsruhe, Germany). Pancreatic peptide YY (PYY) was measured using a human PYY EIA kit from Phoenix Pharmaceuticals (Karlsruhe, Germany). The HOMA-IR was calculated from fasting insulin and glucose with the following equation: $\text{HOMA-IR} = \text{fasting insulin (mIU/mL)} / \text{fasting glucose (mol/L)} / 22.5$.

Intravenous glucose tolerance test

An intravenous glucose tolerance test (IVGTT) was performed as previously described (Soriguer et al., 2009; Garcia-Serrano et al., 2015). The insulin sensitivity index (SI) was calculated after introduction of the results for glucose and insulin obtained during the IVGTT into the MINMOD program (version 3.0, 1994, Richard N. Bergman).

Anthropometric measurements

Body weight, height, waist and hip circumferences were measured according to standardized procedures [16]. BMI was calculated as weight (kilograms) divided by height (meters) squared.

Visceral adipose tissue mRNA

Visceral adipose tissue (VAT) was obtained during bariatric surgery in morbidly obese patients. The biopsy samples were washed in physiological saline buffer and immediately frozen in liquid nitrogen until analysis. Frozen adipose tis-

sue was homogenized with an Ultra-Turrax 8 (Ika, Staufen, Germany). Total RNA was extracted by RNeasy lipid tissue midi kit (QIAGEN Science, Hilden, Germany), and treated with 55 U RNase-free deoxyribonuclease (QIAGEN Science, Hilden, Germany) following the manufacturer's instructions. RNA purity was determined by 260/280 absorbance ratios on a Nanodrop ND-1000 spectrophotometer (Thermo Fisher Scientific Inc. Waltham, MA). Total purified RNA integrity was checked by denaturing agarose gel electrophoresis and ethidium bromide staining. Total RNA was reverse transcribed to cDNA by a high-capacity cDNA reverse transcription kit with RNase inhibitor (Applied Biosystems, Foster City, CA). Quantitative real-time PCR with duplicates was done with the cDNA. The amplifications were performed using a MicroAmpH Optical 96-well reaction plate (Applied Biosystems, Foster City, CA) on an ABI 7500 Fast Real-Time PCR System (Applied Biosystems, Foster City, CA). Commercially available and pre-validated TaqMan® primer/probe sets were used as follows: cyclophilin A (4333763, RefSeq NM_002046.3), used as endogenous control for the target gene in each reaction, TNF alpha (Hs00174128_m1, RefSeq NM_000594.2), IL-6 (Hs00174131_m1, RefSeq NM_000600.2), IL-1 β (Hs00174097_m1, RefSeq NM_000576.2), complement component 3 receptor 3 subunit (CD11b) (Hs01064804_m1, RefSeq NM_000632.3), insulin receptor substrate 1 (IRS-1) (Hs00178563_m1, RefSeq. NM_005544.2), insulin receptor substrate 2 (IRS-2) (Hs00275843_s1, RefSeq. NM_003749.2). A threshold cycle (C_t value) was obtained for each amplification curve and a ΔC_t value was first calculated by subtracting the C_t value for human cyclophilin A cDNA from the C_t value for each sample and transcript. Fold changes compared with the endogenous control were then determined by calculating $2^{-\Delta C_t}$.

RNA extraction from cecal appendix

Total RNA was extracted from cecal appendix samples using a commercially available TriPure Isolation Reagent (Roche) and treated with DNase (RNase-free DNase Set; Qiagen). The RNA concentration was determined by absorbance at 260 nm (A260), and the purity was estimated by determining the A260/A280 ratio with a Nanodrop spectrophotometer (Nanodrop Technologies, Wilmington, DE). Denaturing aga-

Gut microbiota and insulin resistance

Table 1. Biochemical and clinical characteristics of both study groups together with the expression of inflammatory cytokine and macrophage infiltration genes in visceral adipose tissue

	NIR-MO patients N=5	IR-MO patients N=5	*P
Age (years)	48.0±10.5	44.40±8.64	0.570
BMI (kg/m ²)	59.18±4.71	58.20±4.12	0.735
Waist circumference (cm)	146.60±11.71	151.40±14.56	0.580
Hip circumference (cm)	162.67±14.36	162.20±17.03	0.964
SBP (mmHg)	132.00±23.28	141.0±27.87	0.595
DBP (mmHg)	82.40±10.90	86.60±10.13	0.546
Total cholesterol (mg/dl)	211.60±16.34	207.80±18.70	0.741
HDL cholesterol (mg/dl)	51.60±11.80	47.40±11.30	0.581
LDL cholesterol (mg/dl)	130.23±17.67	127.33±19.12	0.810
Triglycerides (mg/dl)	89.04±13.46	159.39±15.9	0.001
Insulin (mg/dl)	8.92±1.74	26.93±3.85	0.001
Glucose (mg/dl)	94.40±4.36	104.80±3.63	0.003
HOMA-IR	2.18±0.53	8.34±1.24	0.001
SI (10 ⁻⁴ min ⁻¹ /(μU/ml)	2.96±2.33	0.84±0.80	0.020
GOT (U/l)	27.50±6.47	20.40±5.77	0.104
GPT (U/l)	39.00±15.05	42.80±16.76	0.716
GGT (U/l)	47.27±16.00	42.20±13.84	0.649
CRP (mg/L)	3.62±0.91	5.82±0.52	0.002
Leptin (ng/ml)	59.25±11.75	95.08±15.88	0.001
Adiponectin (ug/ml)	13.52±3.54	7.44±1.44	0.007
PYY	0.55±0.17	0.34±0.10	0.044
GLP1	88.80±9.67	56.40±11.52	0.001
IL6_V	0.07±0.02	0.27±0.07	0.001
IL1B_V	0.08±0.02	0.28±0.07	0.001
TNF_alpha_V	0.002±0.0009	0.006±0.002	0.004
IRS1_V	0.014±0.001	0.005±0.001	0.001
IRS2_V	0.59±0.15	0.63±0.08	0.633
CD11b_V	0.12±0.04	0.35±0.10	0.001

Values are presented as means ± SD. N=5 subjects per group. DBP, Diastolic blood pressure; SBP, Systolic blood pressure; SI, Insulin sensitivity; GGT, Gamma-glutamyl transferase; GOT, Glutamic oxaloacetic transaminase; GPT, Glutamic pyruvic transaminase; CRP, C-reactive protein. Values are significantly different for *P<0.05.

rose gel electrophoresis and ethidium bromide staining were used in order to check the integrity of total purified RNA. cDNA was synthesized using SuperScript II reverse transcriptase and random hexamer primers as described in the manufacturer's protocol (Invitrogen Corp).

PCR amplification and analysis of 16S rRNA sequences

Variable regions 2-3 of the 16S rRNA gene were amplified using TaKaRa Ex Taq PCR mixture (TA-

KARA Bio USA, Madison, WI) and the PCR primers HDA1 (5'-GAC-TCCTACGGGAGGCAGCAGT-3') and HDA2 (5'-GTATTACCGCGGCTGCTGGCAC-3'). Forward primers were designed with the adaptor A sequence (CGTATCGCCTCCCTCGCGC-CA) plus a key sequence (TCAG) and reverse primers with the adaptor B sequence (CTATGCGCCTTGCCAGC-CCG) plus a key sequence (TCGA). 454-adaptors were included in the forward primer followed by a 10 bp sample-specific Multiplex Identifier (MID). The PCR program was set as follows: 95°C 10 min and 30 cycles of 95°C 1 min, 50°C 1 min, 72°C 1.5 min followed by 72°C for 10 minutes. Agarose gel electrophoresis was performed and PCR products purified twice with Agencourt AMPure Kit (Beckman Coulter, Milan, Italy) and quantified using the Quant-iT™ PicoGreen® dsDNA Assay kit (Invitrogen, Burlington, ON). An equimolar pool was obtained prior to further processing. This equimolar pool was sequenced in a GS Junior 454 platform according to the manufacturer's protocols using Titanium chemistry (Roche Applied Science, Indianapolis, IN).

Bioinformatics analysis

454 pyrosequencing data were analyzed using QIIME 1.8.0 software [17]. Raw reads were first filtered following the 454 amplicon processing pipeline. The pyrosequencing reads were demultiplexed and further filtered through the split_

library.py script of QIIME. Reads with an average quality score lower than 25, ambiguous base calls, primer mismatches or shorter than 100 bp were excluded from the analysis in order to increase the level of accuracy. After the quality filter, the pipeline analysis used to analyze 16S gene reads was the following: sequences were denoised and singletons excluded. Operational taxonomic units (OTUs) were picked by clustering sequences at a similarity of >97% and the representative sequences, chosen as the most abundant in each cluster, were sub-

Table 2. Chao1 richness estimator and Shannon diversity index among microbial communities obtained from appendix samples from IR-MO and NIR-MO patients

	IR-MO patients (n=5)	NIR-MO patients (n=5)	P
Chao 1	99.19±29.03	102.0±36.51	0.89
Shannon	3.69±0.91	3.34±0.92	0.59

The Chao richness estimator and Shannon diversity index were calculated at 3% distance.

mitted to the UCLUST to obtain the taxonomy assignment and the relative abundance of each OTU using the Greengenes 16S rRNA gene database. Alpha and beta diversity were evaluated through QIIME, as described [18].

Statistical analysis

Group abundance was determined with a g-test using the `group_significance.py` script within QIIME in order to test whether the presence/abundance of any OTUs was significantly associated with a specific group. An Anosim statistical test through the `compare_category.py` script of QIIME was performed with a weighted UniFrac distance matrix in order to verify whether there were differences between the two types of patients. Comparisons between the results of the morbidly obese patients with high- and low-insulin-resistance were made with the Mann-Whitney test with a Bonferroni post hoc test. The Spearman correlation coefficients were calculated to estimate the correlations between variables. Statistical analyses were carried out with the statistical software package SPSS version 15.0 (SPSS Inc., Chicago, IL, USA). Values were considered to be statistically significant when $P < 0.05$. The results are given as the mean \pm SD.

Results

Biochemical and clinical characteristics together with gene expression in visceral adipose tissue in both study groups

The metabolic and anthropometric characteristics of the two study groups are shown in **Table 1**. The plasma levels of triglycerides, insulin, glucose, CRP, leptin and the HOMA-IR values were all significantly higher in the IR-MO group than in the NIR-MO group ($P < 0.05$). Conversely, the SI, GLP-1, PYY and adiponectin levels were

significantly higher in the NIR-MO group compared to the IR-MO group ($P < 0.05$).

We also found significantly higher mRNA expression levels in visceral adipose tissue of IL6, IL1B, TNF alpha, IRS2 and CD11b in the IR-MO group as compared with the NIR-MO group ($P < 0.05$). Only the visceral adipose tissue expression levels of IRS1 were significantly higher in the NIR-MO group ($P < 0.05$).

Analysis of the microbial community diversity between the study groups

A total 45,820 good quality 16S rRNA gene sequences with an average of $4,582 \pm 2,674.45$ sequences per sample passed the filters applied through QIIME. To obtain a detailed structural overview of the microbiome of each study subject, an OTU analysis was performed. The microbiota of all appendix samples after QIIME were composed of 1128 OTUs with a relative abundance higher than 1% in at least two samples (97% similarity cut-off).

Prior to assessing alpha and beta diversity measures, samples were rarefied to 302 seq, which corresponded to the lowest number of quality reads obtained from any individual sample in the data set. The IR-MO group had a greater number of OTUs than the NIR-MO group (mean = 303 versus mean = 282, respectively; $P > 0.05$).

The average diversity (Shannon index) and community richness (Chao index) were calculated to estimate the alpha diversity. The Chao and Shannon indices of each group suggested a similar bacterial richness and diversity in the appendix samples from the NIR-MO group compared to those from the IR-MO group, with no significant differences ($P = 0.89$ and $P = 0.59$, respectively) (**Table 2**). The rarefaction curve of observed OTUs calculated at 3% distance started to plateau at approximately 100 reads, suggesting that a higher number of reads per sample would not have provided a more comprehensive catalogue of bacterial taxa.

The unweighted UnifracPCoA Principal analysis based on the relative abundance of OTUs for each sample showed useful information about the phylogenetic relationships in the appendix bacterial microbiota in both study groups. Not all the samples from the IR-MO group were

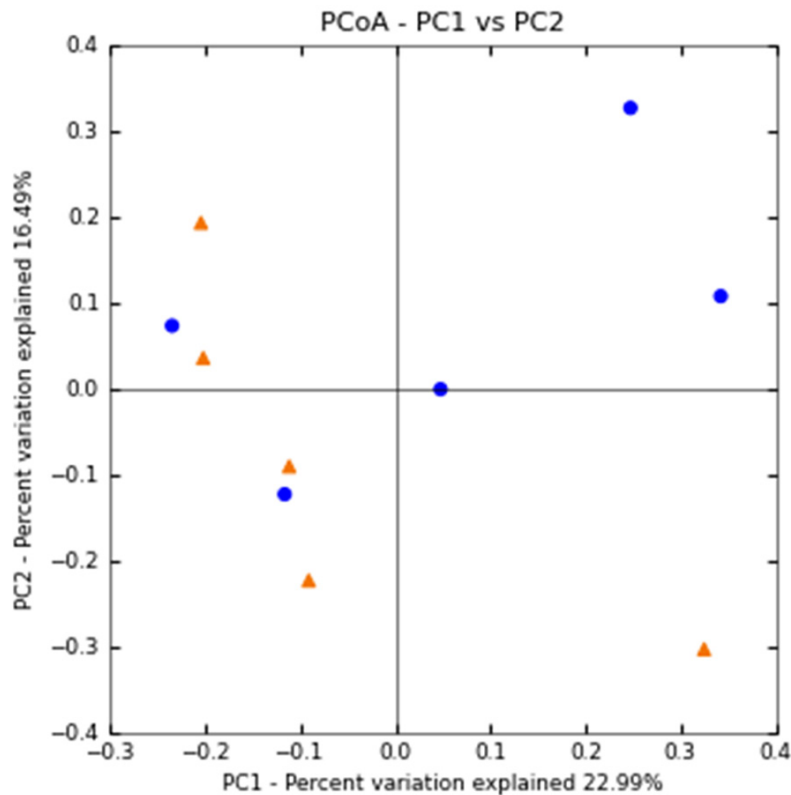


Figure 1. Principal component analysis of bacterial communities from appendix samples subjected to 454 sequencing. Positions of the bacterial communities for each species along the two first principal coordinate axes are illustrated, along with the percentage of variation explained by each axis. Results are based on unweighted Unifrac metrics. IR-MO samples (n=5) represented by red dots; NIR-MO samples (n=5) represented by blue dots.

totally separate from the NIR-MO group in the combinations of coordinates, as demonstrated by the two principal component scores, which accounted for 23% and 16% of total variations. ANOSIM with permutations revealed no significant differences between groups ($P=0.46$), indicating no notable separation between the two groups (**Figure 1**).

16S rRNA gene pyrosequencing of samples from patients with high and low insulin resistance

In this study there were variations in the composition of appendix microbiota in the IR-MO and NIR-MO groups at different bacterial levels. At the phylum level, Firmicutes (47.98% IR vs. 21.45% NIR, $P<0.001$) and Fusobacteria (7.35% IR vs. 1.56% NIR, $P<0.001$) were significantly more abundant in the IR-MO patients, whereas Bacteroidetes (37.25% IR vs. 51.67% NIR, $P=0.02$) and Proteobacteria (7.23% IR vs. 25.90% NIR, $P<0.001$) were significantly pre-

dominant in the NIR-MO patients. The remainder of the bacterial population belonged to 9 other phyla that had a relative abundance lower than 1% (**Figure 2**). In addition, the Firmicutes/Bacteroidetes ratio was significantly different between study groups (1.28% IR vs. 0.41% NIR, $P<0.001$).

Within the 22 families detected among all the groups, 16 families were detected with a relative abundance greater than 1% in at least one group. In the IR-MO group we found a significant increase in Pseudomonaceae (27.83% IR vs. 20.72% NIR, $P<0.001$), Prevotellaceae (7.89% IR vs. 0.46% NIR, $P=0.01$), and moreover in the unique family within the phyla Fusobacteria, Fusobacteriaceae ($P<0.001$); and a significant decrease in the abundance of Bacteroidaceae (49.92% IR vs. 70.41% NIR, $P=0.03$), Lachnospiraceae (36.11% IR vs.

43.26% NIR, $P<0.001$), Ruminococcaceae (34.85% IR vs. 43.61% NIR, $P<0.001$) and Enterobacteriaceae (20.00% IR vs. 36.04% NIR, $P<0.001$). No significant differences between study groups were found in other abundant families, including Erysipelothricaceae (5.56% IR vs. 5.08% NIR, $P=0.064$), Odoribacteraceae (7.25% IR vs. 8.04% NIR, $P=0.659$), Porphyromonadaceae (0.48% IR vs. 2.65% NIR, $P=0.108$), Christensenellaceae (3.03% IR vs. 0.70% NIR, $P=0.783$), Rikenellaceae (34.30% IR vs. 17.53% NIR, $P=0.297$), Alcaligenaceae (20.87% IR vs. 4.68% NIR, $P=0.589$), Succinivibrionaceae (19.13% IR vs. 1.5% NIR, $P=0.982$), Veillonellaceae (14.39% IR vs. 5.08% NIR, $P=0.984$), and Peptococcaceae (1.26% IR vs. 0.53% NIR, $P=0.668$) (**Figure 3**).

We also found significant differences in microbial composition at the genus level between the study groups. A total of 28 genera were identified among the appendix samples, with six significantly different genera between the

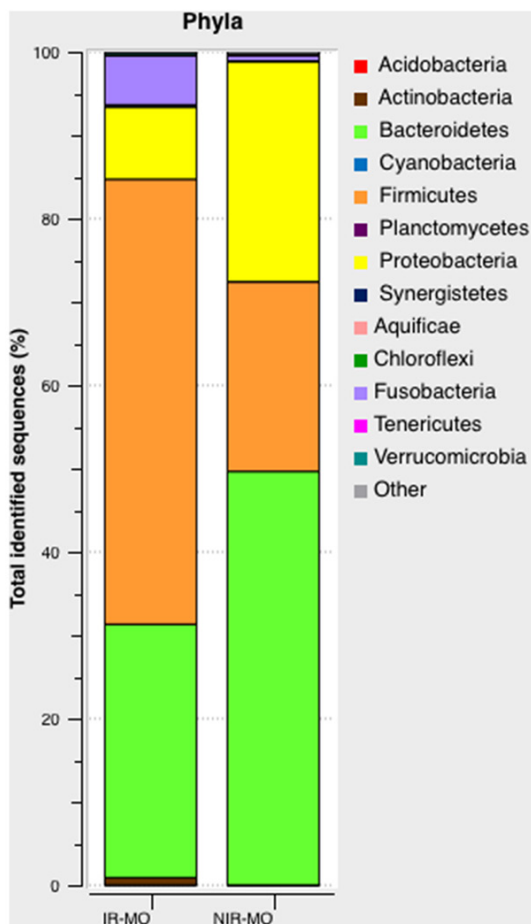


Figure 2. Pyrosequencing analysis of phyla in the IR-MO and NIR-MO groups. Data are shown as a percentage of the total identified sequences per group.

IR-MO and the NIR-MO groups. *Pseudomonas* (27.83% IR vs. 20.72% NIR, $P < 0.001$), *Catenibacterium* (3.54% IR vs. 0.88% NIR, $P = 0.027$), *Prevotella* (7.89% IR vs. 0.46% NIR, $P = 0.01$), *Veillonella* (2.27% IR vs. 0% NIR, $P < 0.001$) and *Fusobacterium* ($P < 0.001$) were significantly greater in the IR-MO group within the constitutive genera over 1% of the phylum bacteria in the appendix samples. On the other hand, *Bacteroides* (49.76% IR vs. 67.85% NIR, $P = 0.05$) and *Blautia* (5.56% IR vs. 8.41% NIR, $P = 0.013$) exhibited a significantly higher abundance in the NIR-MO patients compared to the IR-MO patients. In addition, the genera *Odoribacter* (6.12% IR vs. 5.48% NIR, $P = 0.702$), *Sutterella* (20.87% IR vs. 4.68% NIR, $P = 0.589$), *Succinivibrio* (19.13% IR vs. 0% NIR, $P = 1.000$), *Lachnospira* (2.02% IR vs. 1.75% NIR, $P = 0.356$), *Oscillospira* (4.04% IR vs. 1.05%, $P = 0.770$), and *Ruminococcus* (3.03% IR vs. 0.35% NIR,

$P = 0.637$) dominated the IR-MO group, while *Butyricimonas* (1.13% IR vs. 2.56% NIR, $P = 0.395$), *Parabacteroides* (0.48% IR vs. 2.65% NIR, $P = 0.107$), *Megamonas* (0.25% IR vs. 1.75% NIR, $P = 0.650$) and *Phascolarctobacterium* (1.26% IR vs. 3.33% NIR, $P = 0.956$) dominated the NIR-MO group. Differences in abundance for all these minority genera between the IR-MO and NIR-MO groups were not significant ($P > 0.05$ in all cases) (Figure 4).

QIIME software generally provides confident phylogenetic assignments of DNA sequences down to the taxonomic level of the genus [19]. We were able to detect the following taxa: *Prevotella stercorea*, *Mitsuokella multacida* and *Veillonella disparin* in the IR-MO group.

Relationship between the gut microbiota composition, clinical parameters and inflammatory gene expression in the visceral adipose tissue from both study groups

The IR-MO patients had a significant univariate correlation between the abundance of specific bacterial groups and the plasma glucose levels (*Butyricimonas* $r = -0.918$, $P = 0.028$), plasma insulin levels (*Bifidobacterium* $r = -0.975$, $P = 0.005$), the expression levels of IL6 (*Prevotella* $r = 0.921$, $P = 0.026$), IL1B (*Firmicutes* $r = 0.963$, $P = 0.009$), TNF alpha (*Succinivibrio* $r = 0.975$, $P = 0.005$) and CD11b (*Veillonella* $r = 0.894$, $P = 0.041$). No significant correlation was found in the NIR-MO group ($P < 0.05$).

Discussion

This study is the first to use appendix samples to establish that IR-MO and NIR-MO patients have a specific gut microbial profile using next-generation sequencing technologies. While limited data are available on the microbial composition of the appendix, it has been postulated that this organ could serve as a microbial reservoir for repopulating the gastrointestinal tract in times of necessity [12]. The associated lymphoid tissue of the appendix has been recognized to provide an ideal environment for bacterial growth in biofilms acting as an enteric reservoir [20, 21]. The aforementioned arguments thus strongly suggest the importance of focusing on the appendix microbiota as a novel actor capable of modulating host metabolism via shaping the appendix immune function. In this study, analyzing the relationship between the

Gut microbiota and insulin resistance

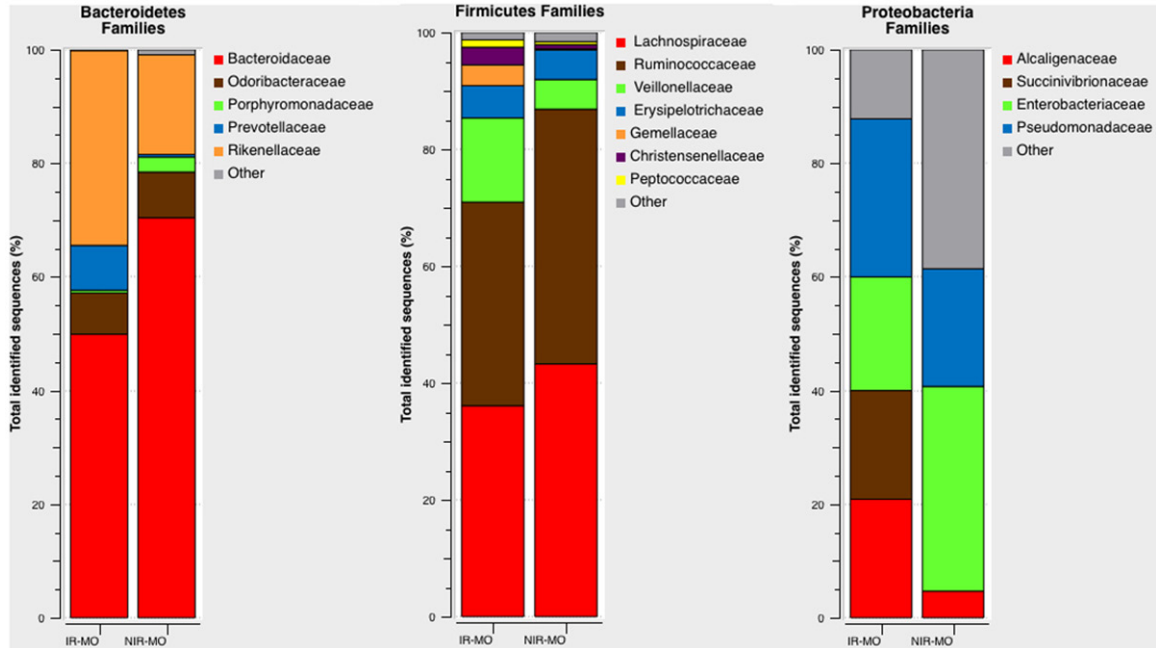


Figure 3. Family-level microbial classification of bacteria from the IR-MO and NIR-MO appendix samples. Data are shown as a percentage of the total identified sequences per group.

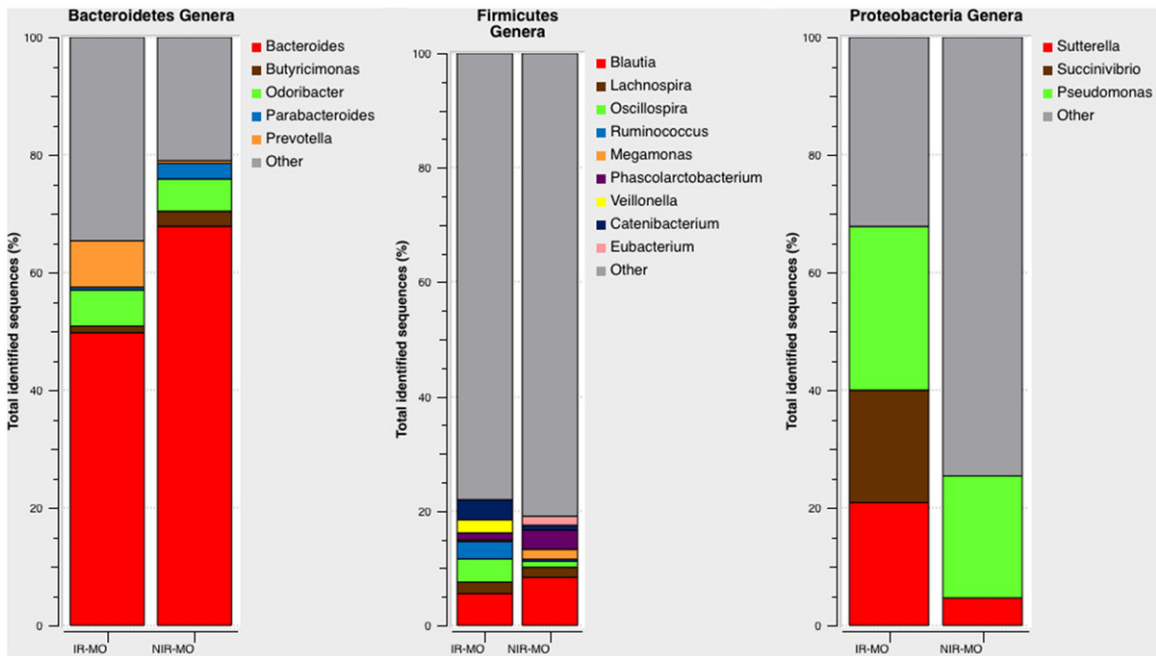


Figure 4. Relative abundance of bacterial genera in the microbiota of the IR-MO and NIR-MO patients. Data are shown as a percentage of the total identified sequences per group.

microbiota composition and insulin resistance in both groups of morbidly obese patients, we considered confounding factors such as BMI, race, gender, age and dietary intake of the study subjects.

Our results indicate that the IR-MO patients have no increased bacterial diversity, as there was no separate cluster when compared to the NIR-MO group, clearly indicated by OTU based PCoA plot. However, the pyrosequencing analy-

sis of the 16S rRNA gene sequences of the relative abundance of predominant phyla, family and genera taxa in the appendix samples revealed large significant differences between the IR-MO and the NIR-MO patients. At the family and genera level, we found that there was a significant increase in the abundance of *Pseudomonaceae*, *Prevotellaceae*, *Fusobacteriaceae*, *Pseudomonas*, *Prevotella*, *Catenibacterium*, *Veillonella*, and *Fusobacterium* and a decrease in *Bacteroidaceae*, *Lachnospiraceae*, *Ruminococcaceae*, *Enterobacteriaceae*, *Bacteroides* and *Blautia* in the appendix samples from the IR-MO group. These results suggest that the dominant microbiota are different in the IR-MO patients with respect to the NIR-MO patients. Alterations in the gut microbiota have also been suggested to occur in other human diseases such as Crohn's disease, ulcerative colitis [22-24], celiac disease in children [25], and allergic inflammation in infants [26]. The morbidly obese patients with an IR microbiota phenotype also had a higher rate of systemic inflammation, with a significant increase in CRP and leptin levels and a decrease in serum adiponectin levels. Recent data have shown that variations in intestinal microbiota are associated with pro-inflammatory changes in adipose gene expression [27]. In this study we also found a significant increase in the expression level of inflammatory markers such as IL6, IL1B and TNF alpha in the VAT of the IR-MO patients. Moreover, there was a significant positive correlation between the abundance of *Prevotella*, *Succinivibrio* and *Firmicutes* and the VAT expression levels of IL6, TNF alpha and IL1B, respectively. Several years ago, Burcellin et al. suggested that a so-called 'metabolic infection' might exist, suggesting that the gut microbiota might be an important factor in low-grade systemic inflammation and the development of insulin resistance. In their study using animal models, the authors demonstrated that prior to the onset of diabetes, and soon after the mice are switched to a high-fat diet, intestinal bacteria translocate from the gut to the adipose tissue and blood, where they might induce low-grade inflammation [28]. In addition, TNF alpha is able to phosphorylate serine residue substrate from the IRS-1, leading to its inactivation [29].

Based on these data, the presence of a local appendix dysbiosis and the inflammation triggered by the intestinal bacteria in the IR-MO

group might be pathological and could be linked to the development of insulin resistance in morbidly obese patients. In accordance with our results, Meadows described that *Firmicutes* are linked to weight gain and insulin resistance because they provide a source of extra calories by breaking down polysaccharides that are otherwise indigestible in mammals [30]. Verdum et al., with results similar to ours, showed that a decrease in *Bacteroidetes* and an increase in *Firmicutes* is associated with the presence of obesity and inflammation in humans [11]. *Fusobacterium* spp. has also been considered a pro-inflammatory passenger bacteria in the origin and proliferation of human colorectal cancer [31].

In this study, the significant increase in the abundance of *Prevotella* suggests an evolution of a mucin-degrading niche in the IR-MO group. Mucin degradation by bacteria is often regarded as an initial stage in pathogenesis [32], since it would disturb the protection of the host mucosal surfaces and potentially lead to a disruption in the epithelial barrier, increasing intestinal permeability, facilitating bacterial translocation and a paracellular flux of lipopolysaccharides (LPS) able to induce inflammation in the host [33, 34], as we thought might possibly occur in the IR-MO patients. In addition, the significant increase in the VAT expression of CD11b in the IR-MO group may be due to this increase in permeability, which would trigger an immune response, inflammation, and immune cell (such as macrophages) infiltration in the adipose tissue. Moreover, we observed a significant positive correlation between the VAT expression of CD11b and the relative abundance of *Veillonella* in the IR-MO group. These bacteria are able to ferment glucose and lactate to propionate, acetate and succinate; however, these short fatty acids do not induce mucin synthesis [35], which could result in a reduction of the tight junction assembly, generating an increase in gut permeability. This situation is able to induce insulin resistance and also reduce the levels of gut-secreted hormones, such as GLP-1 and PYY, as we have described in the IR-MO patients in our study. One possible mechanism to explain the significant decrease in secretion of GLP1 and PYY in the IR-MO patients may be that its secretion is modulated by the short-chain fatty acids (SCFA) produced by the altered gut microbiota. The significant decrease in the abundance of *Lach-*

nospiraceae and *Ruminococcaceae* found in this study in the IR-MO group is very relevant because both families are able to degrade complex polysaccharides to SCFA, including acetate, butyrate, and propionate that can be used for energy by the host [36]. Moreover, these SCFA act as anti-inflammatory molecules, capable of inhibiting NF- κ B activation in the host immune cells by binding to G-protein-coupled receptors (GPR43 and GPR41), thereby blocking inflammatory responses and suppressing TNF alpha and IL6 release [37]. In addition, previous studies have also shown that butyrate induces mucin synthesis [35], decreases bacterial transport across the epithelium [38] and decreases intestinal epithelial permeability by increasing the expression of tight junction proteins [39].

Butyrate producing intestinal bacteria also seem to play an important role in blood glucose regulation and lipid metabolism, as shown by fecal transplantation studies [40]. In the present study we found negative and significant correlations between the abundance of bacteria, such as *Butyricimonas* (butyrate producers with anti-inflammatory effects) and *Bifidobacterium*, and the plasma glucose and insulin levels, respectively, in the IR-MO patients. In previous studies, the levels of *Bifidobacterium* have also been related to improved glucose metabolism, insulin resistance and low-grade inflammation [11, 41]. Furthermore, improved insulin sensitivity was found after infusion of butyrate-producing intestinal microbiota from lean donors to male subjects with the metabolic syndrome [40].

Our results also demonstrate that the abundance of bacteria that can act as opportunistic pathogens, such as *Pseudomonas* and *Sutterella*, was elevated in the appendix samples from the IR-MO patients compared with the NIR-MO patients. Williams *et al.* found high detection rates of *Sutterella* in gastrointestinal biopsies from autistic children with a gastrointestinal disturbance. These authors indicated that it is not yet evident what the consequences of this increase in fecal *Sutterella* population means, but it is possible that under specific conditions these bacteria could cause infection [42]. Previous reports have shown that *Pseudomonadaceae* were significantly increased in the stools of patients with end-

stage renal disease [43] and Geng *et al.* considered the *Pseudomonadaceae* family as a new potential driver bacteria in human colorectal cancer progression [44].

In conclusion, our data support the hypothesis that appendix dysbiosis occurs in the IR-MO group. Moreover, the IR-MO patients showed a loss of butyrate-producing bacteria, essential to maintain gut integrity, together with an increase in mucin-degrading bacteria and opportunistic pathogens. Finally, the significant increase in the expression of inflammatory cytokines and macrophage infiltration genes in adipose tissue, possibly triggered by the microbiota present in the IR-MO group, may suggest that these specific bacteria could initiate the inflammation and the insulin resistance associated with obesity in these patients. These findings could be useful for developing strategies to control the development of insulin resistance by modifying the gut microbiota.

Acknowledgements

This work was supported by grant from the Fondo de Investigación Sanitaria of Instituto de Salud Carlos III and cofounded by Fondo Europeo de Desarrollo Regional FEDER (PI15/01114). The research group belongs to the “Centros de Investigación en Red” [CIBER, CB06/03/0018] of the “Instituto de Salud Carlos III”. Isabel Moreno Indias was supported by a “Sara Borrell” Postdoctoral contract (CD12/00530), Maria Isabel Queipo-Ortuño acknowledges support from the “Miguel Servet Type I” program (CP13/00065) and Fernando Cardona acknowledges support from the “Miguel Servet Type II” program (CP13/00023) from the Instituto de Salud Carlos III, Madrid Spain, co-founded by Fondo Europeo de Desarrollo Regional-FEDER.

Disclosure of conflict of interest

None.

Authors' contribution

MI, SA, GF, CF, QO and FT contributed to the conception, design, analysis, and interpretation of data for the work. MI, SA, GF, CF, QO and FT drafted and revised the intellectual content of the work and approved the final version to be published. They are agreement to be account-

able for all aspects of the work in ensuring that questions related to the accuracy or integrity of any part of the work are appropriately investigated and resolved.

Abbreviations

BMI, body mass index; CRP, high-sensitivity C-reactive protein; DBP, diastolic blood pressure; GLP-1, glucagon-like peptide-1; GPR43 and GPR41, G-protein-coupled receptor; HOMA-IR, homeostasis model assessment of insulin resistance; IL, interleukin; IR-MO, high-insulin-resistant group; IRS-1, insulin receptor substrate; IRS-2, insulin receptor substrate 2; LPS, lipopolysaccharides; NIR-MO, low-insulin-resistant group; OTUs, operational taxonomic units; PCR-DGGE, polymerase chain reaction denaturing gradient gel electrophoresis; PYY, pancreatic peptide YY; SBP, systolic blood pressure; SCFA, short-chain fatty acids; TNF alpha, tumor necrosis factor alpha; VAT, Visceral adipose tissue.

Address correspondence to: Maria Isabel Queipo-Ortuño, Laboratorio de Investigación Biomédica 1ª planta, Instituto de Investigación Biomédica (IBIMA), Complejo Hospitalario de Málaga (Virgen de la Victoria), Campus de Teatinos s/n 29010-Málaga, Spain. Tel: 34/951032647; E-mail: maribelqo@gmail.com

References

- [1] Carvalho BM and Saad MJ. Influence of gut microbiota on subclinical inflammation and insulin resistance. *Mediators Inflamm* 2013; 2013: 986734.
- [2] De Bandt JP, Waligora-Dupriet AJ and Butel MJ. Intestinal microbiota in inflammation and insulin resistance: relevance to humans. *Curr Opin Clin Nutr Metab Care* 2011; 14: 334-340.
- [3] Shoelson SE, Lee J and Goldfine AB. Inflammation and insulin resistance. *J Clin Invest* 2006; 116: 1793-1801.
- [4] Caricilli AM and Saad MJ. The role of gut microbiota on insulin resistance. *Nutrients* 2013; 5: 829-851.
- [5] Stachowicz N and Kiersztan A. [The role of gut microbiota in the pathogenesis of obesity and diabetes]. *Postepy Hig Med Dosw (Online)* 2013; 67: 288-303.
- [6] Tagliabue A and Elli M. The role of gut microbiota in human obesity: Recent findings and future perspectives. *Nutr Metab Cardiovasc Dis* 2013; 23: 160-168.
- [7] Tilg H and Moschen AR. Microbiota and diabetes: an evolving relationship. *Gut* 2014; 63: 1513-21.
- [8] Cani PD, Osto M, Geurts L and Everard A. Involvement of gut microbiota in the development of low-grade inflammation and type 2 diabetes associated with obesity. *Gut Microbes* 2012; 3: 279-288.
- [9] Amar J, Burcelin R, Ruidavets JB, Cani PD, Fauvel J, Alessi MC, Chamontin B and Ferrieres J. Energy intake is associated with endotoxemia in apparently healthy men. *Am J Clin Nutr* 2008; 87: 1219-1223.
- [10] Cani PD, Possemiers S, Van de Wiele T, Guiot Y, Everard A, Rottier O, Geurts L, Naslain D, Neyrinck A, Lambert DM, Muccioli GG and Delzenne NM. Changes in gut microbiota control inflammation in obese mice through a mechanism involving GLP-2-driven improvement of gut permeability. *Gut* 2009; 58: 1091-1103.
- [11] Verdam FJ, Fuentes S, de Jonge C, Zoetendal EG, Erbil R, Greve JW, Buurman WA, de Vos WM and Rensen SS. Human intestinal microbiota composition is associated with local and systemic inflammation in obesity. *Obesity (Silver Spring)* 2013; 21: E607-615.
- [12] Randal Bollinger R, Barbas AS, Bush EL, Lin SS and Parker W. Biofilms in the large bowel suggest an apparent function of the human vermiform appendix. *J Theor Biol* 2007; 249: 826-831.
- [13] Rhee KJ, Jasper PJ, Sethupathi P, Shanmugam M, Lanning D and Knight KL. Positive selection of the peripheral B cell repertoire in gut-associated lymphoid tissues. *J Exp Med* 2005; 201: 55-62.
- [14] Guinane CM, Tadrous A, Fouhy F, Ryan CA, Dempsey EM, Murphy B, Andrews E, Cotter PD, Stanton C and Ross RP. Microbial composition of human appendices from patients following appendectomy. *MBio* 2013; 4.
- [15] Serino M, Fernandez-Real JM, Garcia-Fuentes E, Queipo-Ortuno M, Moreno-Navarrete JM, Sanchez A, Burcelin R and Tinahones F. The gut microbiota profile is associated with insulin action in humans. *Acta Diabetol* 2013; 50: 753-761.
- [16] Lohman TG, Roche AF and Martorell R. Anthropometric standardization reference manual. Champaign, IL: Human Kinetics Books; 1988.
- [17] Caporaso JG, Kuczynski J, Stombaugh J, Bittinger K, Bushman FD, Costello EK, Fierer N, Pena AG, Goodrich JK, Gordon JL, Huttley GA, Kelley ST, Knights D, Koenig JE, Ley RE, Lozupone CA, McDonald D, Muegge BD, Pirrung M, Reeder J, Sevinsky JR, Turnbaugh PJ, Walters WA, Widmann J, Yatsunenkov T, Zaneveld J and Knight R. QIIME allows analysis of high-throughput community sequencing data. *Nat Meth* 2010; 7: 335-336.
- [18] De Filippis F, La Stora A, Villani F and Ercolani D. Exploring the sources of bacterial spoilers in beefsteaks by culture-independent high-

Gut microbiota and insulin resistance

- throughput sequencing. *PLoS One* 2013; 8: e70222.
- [19] Cole JR, Wang Q, Cardenas E, Fish J, Chai B, Farris RJ, Kulam-Syed-Mohideen AS, McGarrell DM, Marsh T, Garrity GM and Tiedje JM. The Ribosomal Database Project: improved alignments and new tools for rRNA analysis. *Nucleic Acids Res* 2009; 37: D141-145.
- [20] Bollinger RR, Barbas AS, Bush EL, Lin SS, Lin SS and Parker W. Biofilms in the normal human large bowel: fact rather than fiction. *Gut* 2007; 56: 1481-1482.
- [21] Bollinger RR, Everett ML, Palestrant D, Love SD, Lin SS and Parker W. Human secretory immunoglobulin A may contribute to biofilm formation in the gut. *Immunology* 2003; 109: 580-587.
- [22] Frank DN, St Amand AL, Feldman RA, Boedeker EC, Harpaz N and Pace NR. Molecular-phylogenetic characterization of microbial community imbalances in human inflammatory bowel diseases. *Proc Natl Acad Sci U S A* 2007; 104: 13780-13785.
- [23] Willing B, Halfvarson J, Dicksved J, Rosenquist M, Järnerot G, Engstrand L, Tysk C and Jansson JK. Twin studies reveal specific imbalances in the mucosa-associated microbiota of patients with ileal Crohn's disease. *Inflamm Bowel Dis* 2009; 15: 653-660.
- [24] Willing BP, Dicksved J, Halfvarson J, Andersson AF, Lucio M, Zheng Z, Järnerot G, Tysk C, Jansson JK and Engstrand L. A pyrosequencing study in twins shows that gastrointestinal microbial profiles vary with inflammatory bowel disease phenotypes. *Gastroenterology* 2010; 139: 1844-1854, e1841.
- [25] Nadal I, Donat E, Ribes-Koninckx C, Calabuig M and Sanz Y. Imbalance in the composition of the duodenal microbiota of children with coeliac disease. *J Med Microbiol* 2007; 56: 1669-1674.
- [26] Kalliomaki M and Isolauri E. Role of intestinal flora in the development of allergy. *Curr Opin Allergy Clin Immunol* 2003; 3: 15-20.
- [27] Kong LC, Tap J, Aron-Wisnewsky J, Pelloux V, Basdevant A, Bouillot JL, Zucker JD, Doré J and Clément K. Gut microbiota after gastric bypass in human obesity: increased richness and associations of bacterial genera with adipose tissue genes. *Am J Clin Nutr* 2013; 98: 16-24.
- [28] Amar J, Chabo C, Waget A, Klopp P, Vachoux C, Bermudez-Humaran LG, Smirnova N, Berge M, Sulpice T, Lahtinen S, Ouwehand A, Langella P, Rautonen N, Sansonetti PJ and Burcelin R. Intestinal mucosal adherence and translocation of commensal bacteria at the early onset of type 2 diabetes: molecular mechanisms and probiotic treatment. *EMBO Mol Med* 2011; 3: 559-572.
- [29] Cani PD and Delzenne NM. The role of the gut microbiota in energy metabolism and metabolic disease. *Curr Pharm Des* 2009; 15: 1546-1558.
- [30] Meadows R. Gut Bacteria May Override Genetic Protections against Diabetes. *PLoS Biol* 2011; 9: e1001215.
- [31] Tjalsma H, Boleij A, Marchesi JR and Dutilh BE. A bacterial driver-passenger model for colorectal cancer: beyond the usual suspects. *Nat Rev Microbiol* 2012; 10: 575-582.
- [32] Derrien M, van Passel MW, van de Bovenkamp JH, Schipper RG, de Vos WM and Dekker J. Mucin-bacterial interactions in the human oral cavity and digestive tract. *Gut Microbes* 2010; 1: 254-268.
- [33] Bischoff SC, Barbara G, Buurman W, Ockhuizen T, Schulzke JD, Serino M, Tilg H, Watson A and Wells JM. Intestinal permeability—a new target for disease prevention and therapy. *BMC Gastroenterol* 2014; 14: 189.
- [34] Moreno-Indias I, Cardona F, Tinahones FJ and Queipo-Ortuno MI. Impact of the gut microbiota on the development of obesity and type 2 diabetes mellitus. *Front Microbiol* 2014; 5: 190.
- [35] Burger-van Paassen N, Vincent A, Puiman PJ, van der Sluis M, Bouma J, Boehm G, van Goudoever JB, van Seuning I and Renes IB. The regulation of intestinal mucin MUC2 expression by short-chain fatty acids: implications for epithelial protection. *Biochem J* 2009; 420: 211-219.
- [36] Biddle A, Stewart L, Blanchard J and Leschine S. Untangling the Genetic Basis of Fibrolytic Specialization by Lachnospiraceae and Ruminococcaceae in Diverse Gut Communities. *Diversity* 2013; 5: 627-640.
- [37] Lewis K, Lutgendorff F, Phan V, Soderholm JD, Sherman PM and McKay DM. Enhanced translocation of bacteria across metabolically stressed epithelia is reduced by butyrate. *Inflamm Bowel Dis* 2010; 16: 1138-1148.
- [38] Peng L, Li ZR, Green RS, Holzman IR and Lin J. Butyrate enhances the intestinal barrier by facilitating tight junction assembly via activation of AMP-activated protein kinase in Caco-2 cell monolayers. *J Nutr* 2009; 139: 1619-1625.
- [39] Udayappan SD, Hartstra AV, Dallinga-Thie GM and Nieuwdorp M. Intestinal microbiota and faecal transplantation as treatment modality for insulin resistance and type 2 diabetes mellitus. *Clin Exp Immunol* 2014; 177: 24-29.
- [40] Vrieze A, Van Nood E, Holleman F, Salojarvi J, Kootte RS, Bartelsman JF, Dallinga-Thie GM, Ackermans MT, Serlie MJ, Oozeer R, Derrien M, Druesne A, Van Hylckama Vlieg JE, Bloks VW, Groen AK, Heilig HG, Zoetendal EG, Stroe ES, de Vos WM, Hoekstra JB and Nieuwdorp M.

Gut microbiota and insulin resistance

- Transfer of intestinal microbiota from lean donors increases insulin sensitivity in individuals with metabolic syndrome. *Gastroenterology* 2012; 143: 913-916, e917.
- [41] Philippe D, Favre L, Foata F, Adolfsson O, Perruisseau-Carrier G, Vidal K, Reuteler G, Dayer-Schneider J, Mueller C and Blum S. *Bifidobacterium lactis* attenuates onset of inflammation in a murine model of colitis. *World J Gastroenterol* 2011; 17: 459-469.
- [42] Williams BL, Hornig M, Parekh T and Lipkin WI. Application of novel PCR-based methods for detection, quantitation, and phylogenetic characterization of *Sutterella* species in intestinal biopsy samples from children with autism and gastrointestinal disturbances. *MBio* 2012; 3.
- [43] Vaziri ND, Wong J, Pahl M, Piceno YM, Yuan J, DeSantis TZ, Ni Z, Nguyen TH and Andersen GL. Chronic kidney disease alters intestinal microbial flora. *Kidney Int* 2013; 83: 308-315.
- [44] Geng J, Song Q, Tang X, Liang X, Fan H, Peng H, Guo Q and Zhang Z. Co-occurrence of driver and passenger bacteria in human colorectal cancer. *Gut Pathogens* 2014; 6: 26-26.